

FIGURE 3 Comparison between simulated grayscale maps and real HFA 10-2 results of in three cases of glaucoma. The grayscale maps show the simulated visual field (VF) (A, C, E) and real VF (B, D, F). (A, B) Case 1. (C, D) Case 2. (E, F) Case 3.

In conclusion, we found that there were significant correlation between structure and function in the macular area, which enabled us to create simulated visual fields from RNFLT data with a high degree of similarity to actual visual fields. Such a simulation of macular function, derived from OCT parameters, may be of help in assessments of glaucoma, particularly in assessments of patients

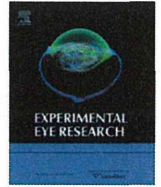
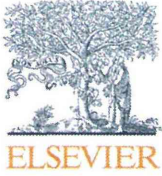
who have difficulty undergoing actual visual field examinations.

**DECLARATION OF INTEREST**

The authors report no conflict of interest.

## REFERENCES

1. Quigley HA. Number of people with glaucoma worldwide. *Br J Ophthalmol* 1996;80:389–393.
2. Quigley HA, Broman AT. The number of people with glaucoma worldwide in 2010 and 2020. *Br J Ophthalmol* 2006;90:262–267.
3. Quigley HA, Dunkelberger GR, Green WR. Retinal ganglion cell atrophy correlated with automated perimetry in human eyes with glaucoma. *Am J Ophthalmol* 1989;107:453–464.
4. Huang D, Swanson EA, Lin CP, Schuman JS, Stinson WG, Chang W, et al. Optical coherence tomography. *Science* 1991;254:1178–1181.
5. Guedes V, Schuman JS, Hertzmark E, Wollstein G, Correnti A, Mancini R, et al. Optical coherence tomography measurement of macular and nerve fiber layer thickness in normal and glaucomatous human eyes. *Ophthalmology* 2003;110:177–189.
6. Greenfield DS, Bagga H, Knighton RW. Macular thickness changes in glaucomatous optic neuropathy detected using optical coherence tomography. *Arch Ophthalmol* 2003;121:41–46.
7. Lederer DE, Schuman JS, Hertzmark E, Heltzer J, Velazques LJ, Fujimoto JG, et al. Analysis of macular volume in normal and glaucomatous eyes using optical coherence tomography. *Am J Ophthalmol* 2003;135:838–843.
8. Wollstein G, Schuman JS, Price LL, Aydin A, Beaton SA, Stark PC, et al. Optical coherence tomography (OCT) macular and peripapillary retinal nerve fiber layer measurements and automated visual fields. *Am J Ophthalmol* 2004;138:218–225.
9. Mwanza JC, Oakley JD, Budenz DL, Chang RT, Knight OJ, Feuer WJ. Macular ganglion cell-inner plexiform layer: automated detection and thickness reproducibility with spectral domain-optical coherence tomography in glaucoma. *Invest Ophthalmol Vis Sci* 2011;52:8323–8329.
10. Kim NR, Lee ES, Seong GJ, Kim JH, An HG, Kim CY. Structure-function relationship and diagnostic value of macular ganglion cell complex measurement using Fourier-domain OCT in glaucoma. *Invest Ophthalmol Vis Sci* 2010;51:4646–4651.
11. Seong M, Sung KR, Choi EH, Kang SY, Cho JW, Um TW, et al. Macular and peripapillary retinal nerve fiber layer measurements by spectral domain optical coherence tomography in normal-tension glaucoma. *Invest Ophthalmol Vis Sci* 2010;51:1446–1452.
12. Omodaka K, Nakazawa T, Yokoyama Y, Doi H, Fuse N, Nishida K. Correlation between peripapillary macular fiber layer thickness and visual acuity in patients with open-angle glaucoma. *Clin Ophthalmol* 2010;4:629–635.
13. Anderson DR, Patella VM. *Automated static perimetry*. 2nd ed. St. Louis: Mosby; 1999.
14. Pavlidis M, Stupp T, Naskar R, Cengiz C, Thanos S. Retinal ganglion cells resistant to advanced glaucoma: a postmortem study of human retinas with the carbocyanine dye DiI. *Invest Ophthalmol Vis Sci* 2003;44:5196–5205.
15. Kang SH, Hong SW, Im SK, Lee SH, Ahn MD. Effect of myopia on the thickness of the retinal nerve fiber layer measured by Cirrus HD optical coherence tomography. *Invest Ophthalmol Vis Sci* 2010;51:4075–4083.
16. Leung CK, Yu M, Weinreb RN, Ye C, Liu S, Lai G, et al. Retinal nerve fiber layer imaging with spectral-domain optical coherence tomography: a prospective analysis of age-related loss. *Ophthalmology* 2012;119:731–737.
17. Drasdo N, Millican CL, Katholi CR, Curcio CA. The length of Henle fibers in the human retina and a model of ganglion receptive field density in the visual field. *Vision Res* 2007;47:2901–2911.
18. Raza AS, Cho J, de Moraes CG, Wang M, Zhang X, Kardon RH, et al. Retinal ganglion cell layer thickness and local visual field sensitivity in glaucoma. *Arch Ophthalmol* 2011;129:1529–1536.



## Comparison of CCD-equipped laser speckle flowgraphy with hydrogen gas clearance method in the measurement of optic nerve head microcirculation in rabbits

Hiroaki Takahashi<sup>a</sup>, Tetsuya Sugiyama<sup>b,\*</sup>, Hideki Tokushige<sup>a</sup>, Takatoshi Maeno<sup>c</sup>, Toru Nakazawa<sup>d</sup>, Tsunehiko Ikeda<sup>b</sup>, Makoto Araie<sup>e</sup>

<sup>a</sup> Research Laboratory for Drug Development, Senju Pharmaceutical Co., Ltd., 1-5-4 Murotani, Nishi-ku, Kobe, Hyogo 651-2241, Japan

<sup>b</sup> Department of Ophthalmology, Osaka Medical College, 2-7 Daigaku-machi, Takatsuki, Osaka 569-8686, Japan

<sup>c</sup> Department of Ophthalmology, Toho University Sakura Medical Center, 564-1 Shimoshizu, Sakura, Chiba 285-8741, Japan

<sup>d</sup> Department of Ophthalmology, Tohoku University Graduate School of Medicine, 1-1 Seiryō-machi, Aoba-ku, Sendai, Miyagi 980-8574, Japan

<sup>e</sup> Kanto Central Hospital of The Mutual Aid Association of Public School Teachers, 6-25-1 Kamiyoga, Setagaya-ku, Tokyo 158-0098, Japan

### ARTICLE INFO

#### Article history:

Received 6 October 2012

Accepted in revised form 10 December 2012

Available online 19 December 2012

#### Keywords:

optic nerve head  
laser speckle flowgraphy  
mean blur rate  
hydrogen gas clearance method  
capillary blood flow  
rabbit

### ABSTRACT

The aim of this study was to verify the correlation between mean blur rate (MBR) obtained with CCD-equipped laser speckle flowgraphy (LSFG) and capillary blood flow (CBF) obtained by the hydrogen gas clearance method in rabbit optic nerve head (ONH). Using Japanese white rabbits under systemic anesthesia, a hydrogen electrode was inserted an area of the ONH free from superficial capillaries. MBR was measured with LSFG near the hydrogen electrode. CBF and MBR were measured in the range of 32.4–83.5 mL/min/100 g and 3.5–6.0, respectively. MBR and CBF were significantly correlated ( $r = 0.73$ ,  $P < 0.01$ ,  $n = 14$ ). After inhalation of carbon dioxide (CO<sub>2</sub>) or intravenous administration of endothelin-1 (ET-1), MBR and CBF were changed in the relative range of 0.74–1.27 and 0.76–1.35, respectively. The relative changes in MBR and CBF induced by CO<sub>2</sub> and ET-1 were also significantly correlated ( $r = 0.67$ ,  $P < 0.01$ ). The current results suggest that MBR may correlate with CBF and also change with CBF, as an index of blood flow in the ONH, linearly.

© 2012 Elsevier Ltd. All rights reserved.

### 1. Introduction

Abnormal blood flow regulation is widely recognized to contribute to the pathophysiology of ocular diseases such as glaucoma (Grieshaber et al., 2007; Moore et al., 2008; Pemp et al., 2009). Circulatory factors in the retrobulbar arteries may be associated with the progression of visual field defects in patients with normal-tension glaucoma (Yamazaki and Drance, 1997). Progressive structural changes in the optic nerve head (ONH) also have been related to abnormal ocular blood flow in glaucoma patients (Harris et al., 2008b). For example, Logan et al. (2004) found lower levels of retinal blood flow in abnormal segments of the ONH than in a corresponding normal segment in glaucoma patients. In addition, glaucoma patients with normal rim segments demonstrated lower

retinal blood flow than controls at each location sampled. However, the role played by blood flow and ischemia on the ONH and retina in glaucoma has not yet been clarified, in part because technical difficulties have limited the accurate measurement of ocular blood flow in relevant vascular beds (Caprioli and Coleman, 2010; Harris et al., 2008a).

The Association for Ocular Circulation (<http://www.obfra.org/>) has published consensus reports on ocular circulation measurement methods such as laser Doppler flowmetry (Riva et al., 2010), laser speckle flowgraphy (LSFG) (Sugiyama et al., 2010), retinal vessel analysis (Garhofer et al., 2010), and color Doppler imaging (Stalmans et al., 2011). Among them, LSFG is the only method available to measure tissue circulation non-invasively and provide a 2-dimensional map of ocular tissue circulation. Normalized blur (NB) was the value used previously in LSFG and represents an index of blood velocity (Tamaki et al., 1994, 1995). *In vitro*, NB demonstrated a good linear correlation with the mean velocity of blood cells flowing through a glass capillary tube (calculated from the blood flow rate generated by a calibrated peristaltic pump) (Nagahara et al., 1999) and with the speed of rotation of a ground-

**Abbreviations:** CBF, capillary blood flow; LSFG, laser speckle flowgraphy; MBR, mean blur rate; ONH, optic nerve head.

\* Corresponding author. Tel.: +81 72 683 1221; fax: +81 72 681 8195.

**E-mail addresses:** [tsugiyama@poh.osaka-med.ac.jp](mailto:tsugiyama@poh.osaka-med.ac.jp), [tsugiyama7@gmail.com](mailto:tsugiyama7@gmail.com) (T. Sugiyama).

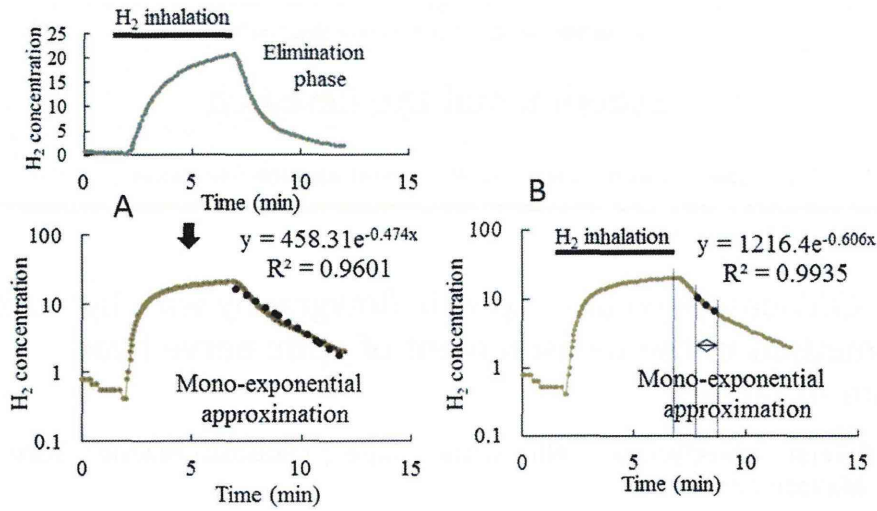


**Fig. 1.** An example of analyzing hydrogen clearance curve to obtain capillary blood flow (CBF) by the hydrogen gas clearance method. The hydrogen concentration was plotted into logarithm (A). The half-life ( $T_{1/2}$ ) at 1–2 min after stopping hydrogen inhalation was adopted for calculation because the linearity of hydrogen clearance in logarithm was the highest there (B). We then calculate CBF as  $69.3/T_{1/2}$  (ml/min/100 g).

glass disc (calculated from the velocity of diffusing particles, which are models of blood cells, on the glass) (Nagahara et al., 1999; Tamaki et al., 1994, 1995, ). *In vivo*, NB was well correlated with tissue blood flow rates determined using the microsphere method in the retina, choroid, or iris, as well as blood flow rates determined with the hydrogen gas clearance method in the ONH (Sugiyama et al., 1996; Takayama et al., 2003; Tamaki et al., 1994, 1995, 1996, 2003; Tomidokoro et al., 1998; Tomita et al., 1999).

In 2008, LSF<sub>G</sub>-NAV<sub>I</sub><sup>TM</sup> was approved as a medical apparatus by the Pharmaceuticals and Medical Devices Agency in Japan. It has adopted a new index: mean blur rate (MBR), the relative velocity index of erythrocytes (Konishi et al., 2002; Watanabe et al., 2008). Recently, Aizawa et al. (2011) reported that MBR has high reproducibility in normal and glaucoma subjects. However, no reports to date have investigated whether MBR is correlated with blood flow rate in the ONH.

The hydrogen gas clearance technique provides multiple capillary blood flow (CBF) measurements quantitatively over long periods of time (Aukland et al., 1964; Csete et al., 2004; Srinivasan

et al., 2011). In the ophthalmic field, this technique has been applied to the ONH in rhesus monkeys (Ernest, 1976) and demonstrated high reproducibility in the measurement of CBF in rabbit ONH (Sugiyama et al., 1995). However, use of this technique is limited to laboratory research because it is highly invasive. The aim of the current study was to verify the correlation between MBR obtained by LSF<sub>G</sub> and CBF obtained by the hydrogen gas clearance method in the rabbit ONH.

**2. Materials and methods**

**2.1. Animals**

Eighteen male Japanese white rabbits weighing 2.5–3.3 kg were purchased from Kitayama Lab. (Nagano, Japan) for the current study. They were housed in an air-conditioned room at temperature of  $23 \pm 3$  °C and humidity of  $55 \pm 10\%$  with a 12-h light–dark cycle and provided with tap water *ad libitum* throughout the experimental period. All animal studies were performed in accordance with the ARVO statement for the use of animals in ophthalmic and vision research and with the approval of the Institutional Animal Care and Use Committee of Kobe Creative Center, Senju Pharmaceutical Co., Ltd.

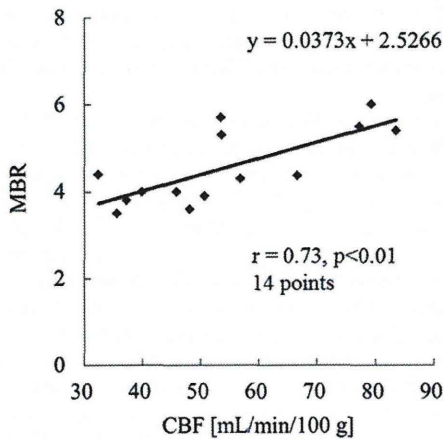


**Fig. 2.** Correlation between the absolute values of CBF and MBR at baseline. CBF and MBR were obtained by the hydrogen gas clearance method and LSF<sub>G</sub>, respectively. Each point represents 1 of 14 different rabbits. Correlation coefficient ( $r$ ) was 0.73 ( $P < 0.01$ ).

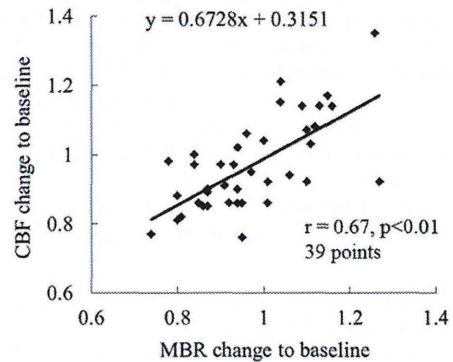


**Fig. 3.** Correlation between the relative changes in CBF and MBR after treatment with CO<sub>2</sub> and ET-1. Each point represents the ratio of relative values to baseline values. Total points were obtained from 39 time points ( $n = 9$  and 6 for CO<sub>2</sub> and ET-1, respectively) in 10 eyes of 14 rabbits. Correlation coefficient ( $r$ ) was 0.67 ( $P < 0.01$ ).

**Table 1**

Distributions of variances by randomized block ANOVA regarding individuality and time-course changes after each treatment.

Treatment	Individuality		Time-course changes	
	CBF	MBR	CBF	MBR
CO <sub>2</sub>	569.268 (8)*	15.046 (8)*	68.750 (3)*	1.358 (3)*
ET-1	262.346 (5)*	1.834 (5)*	11.056 (2)	0.127 (2)

Asterisks represent significant differences ( $P < 0.05$ ) among values obtained from individual rabbits or values at different time points. Degrees of freedom were shown in parentheses.

## 2.2. Measurement of CBF in ONH

Mydriasis was induced by topical tropicamide (Mydrin<sup>®</sup>-M ophthalmic solution 0.4%, Santen Pharmaceutical Co. Ltd., Osaka, Japan). Animals were anesthetized by intraperitoneal injection of 0.8 mg/kg urethane at 0.4 g/mL (Nakalai, Kyoto, Japan) and additional intramuscular injection of 0.1 mg/kg urethane as necessary. Topical anesthesia was induced by topical oxybuprocaine (Benoxil<sup>®</sup> ophthalmic solution 0.4%, Santen Pharmaceutical Co. Ltd.). The CBF in the ONH was measured by the hydrogen gas clearance method as previously reported (Sugiyama et al., 1996). A hydrogen electrode (Cat.# OA211-013, platinum needle with a 0.7-mm long and 0.1-mm diameter Pt-Ir tip, Unique Medical Co., Ltd., Tokyo, Japan) was inserted into a lower portion of the ONH with no visible surface vessels through the vitreous body from the pars plana using a vitrectomy lens. The reference electrode was subcutaneously fixed on the head. After the inhalation of 10% hydrogen gas by a mask at 5 L/min for 5 min, CBF was calculated with the hydrogen concentration half-life ( $T_{1/2}$ ) using a hydrogen clearance flow meter (model MDH-D1, Unique Medical Co., Ltd.). As shown in Fig. 1A, since the clearance curve is approximately mono-exponential, the hydrogen concentration was plotted into logarithm to get half-life ( $T_{1/2}$ ) for calculation. Specifically in the current study, the linearity of hydrogen clearance in logarithm was found beforehand to be the highest at 1–2 min after stopping hydrogen inhalation (Fig. 1B), therefore we adopted the half-life there to calculate CBF as  $69.3/T_{1/2}$  (mL/min/100 g).

## 2.3. Measurement method of MBR in ONH

MBR was measured with a LSF-NAVI-MRC™ device (Softcare Ltd., Iizuka, Japan). The LSF-NAVI-MRC™ consisted of a fundus camera equipped with a diode laser (wavelength: 830 nm) and a CCD image sensor (750 × 360 pixels). The principle and application of this method have been described previously (Konishi et al., 2002; Sugiyama et al., 2010; Tamaki et al., 1995). The measurement area of MBR was designated as a square area free of visible surface vessels near the hydrogen electrode in the ONH.

## 2.4. Measurements of CBF and MBR before and after altering ONH blood flow

To check their stability in measuring ONH blood flow, CBF and MBR were recorded 3 times at 15-min intervals and 5 times at 5-min intervals, respectively. The intervals were recommended in

previous reports (Sugiyama and Azuma, 1995; Tamaki et al., 1995). The inclusion criterion for the stability of measurements was a coefficient of variance (CV) of CBF within 0.1. Averages of measurement values were adopted as baseline values. The correlation between the baseline values of CBF and MBR was estimated. Baseline values were measured before the inhalation of carbon dioxide (CO<sub>2</sub>) or intravenous administration of endothelin-1 (ET-1).

Immediately, 15, and 30 min after 5-min inhalation of 10% CO<sub>2</sub> in ordinary air via mask at 5 L/min, CBF and MBR were measured simultaneously in the same rabbit. CBF was measured once at each time point. MBR was recorded 5 times at each time point, and then the mean value was calculated. Human ET-1 (Peptide Institute, Osaka, Japan) was dissolved in 0.1% aqueous acetic acid to provide a 10<sup>-4</sup> mol/L concentration and diluted with saline for a 10<sup>-6</sup> mol/L solution. CBF and MBR were measured, as above, at 30 min and 1 h after intravenous injection (10<sup>-10</sup> mol/kg) of the prepared ET-1 solution. The relative change in CBF and MBR was calculated by dividing by the baseline value. The expiratory CO<sub>2</sub> density and arterial O<sub>2</sub> and CO<sub>2</sub> pressure were not monitored.

## 2.5. Statistical analysis

Correlation analysis between CBF and MBR was performed using Ekuseru-Toukei 2008 statistical software (Social Survey Research Information Co., Ltd., Tokyo, Japan). We analyzed the effects of each treatment (namely, CO<sub>2</sub> and ET-1) on MBR and CBF by randomized block ANOVA with individual animals as a block using JMP software (Ver. 9.0.0, SAS Institute, Cary, NC). Findings of  $P < 0.05$  were considered significant.

## 3. Results

### 3.1. Correlation between the baseline values of CBF and MBR

A plot of baseline CBF and MBR values is shown in Fig. 2. In 17 of 18 rabbits, the CV of CBF was within 0.1. For measurement of MBR in 3 of 17 rabbits, the square area could not be designated free from visible surface vessels near the hydrogen electrode in the ONH. Therefore, data from 14 eyes of 14 rabbits were used for this analysis. CBF and MBR were measured in the range (mean ± SE) of 32.4–83.5 (54.3 ± 4.5) mL/min/100 g and 3.5–6.0 (4.6 ± 0.2), respectively. A significant positive correlation between the absolute CBF and MBR baseline values was observed ( $r = 0.73$ ,  $P < 0.01$ ,  $n = 14$ ).

### 3.2. Correlation between the relative change in CBF and MBR induced by inhalation of CO<sub>2</sub> and intravenous administration of ET-1

CBF was altered after inhalation of CO<sub>2</sub> or intravenous administration of ET-1. Relative values of CBF changed in the range of 0.74–1.27. MBR in the ONH was also altered. Relative values of MBR changed in the range of 0.76–1.35. A plot of relative changes in CBF and MBR is shown in Fig. 3. In 10 of 14 rabbits, the changes in CBF and MBR induced by CO<sub>2</sub> ( $n = 9$ ) and ET-1 ( $n = 6$ ) were measured with the hydrogen gas clearance method and LSF, respectively. The relative changes in CBF and MBR demonstrated a significant positive correlation ( $r = 0.67$ ,  $P < 0.01$ ).

**Table 2**

Average changes in CBF and MBR after inhalation of CO<sub>2</sub>.

	Baseline levels	Immediately	15 min	30 min
CBF (mL/min/100 g)	50.7 ± 11.5	52.3 ± 12.1 (1.04 ± 0.11)	48.3 ± 14.2 (0.95 ± 0.14)	46.0 ± 11.4* (0.91 ± 0.10)
MBR	4.7 ± 2.0	5.0 ± 2.0* (1.08 ± 0.10)	4.6 ± 2.5 (0.97 ± 0.13)	4.0 ± 1.4* (0.89 ± 0.08)

Data are expressed as mean ± SD for 9 rabbits. Asterisks represent significant differences ( $P < 0.05$ ) compared to baseline levels by paired *t*-test. CBF/MBR changes to baseline levels were shown in parentheses.

**Table 3**  
Average changes in CBF and MBR after intravenous administration of ET-1.

	Baseline levels	30 min	60 min
CBF (mL/min/100 g)	41.6 ± 10.2	41.9 ± 9.8 (1.02 ± 0.15)	39.4 ± 10.5 (0.95 ± 0.16)
MBR	4.1 ± 0.8	3.9 ± 1.0 (0.95 ± 0.08)	3.9 ± 0.7 (0.95 ± 0.20)

Data are expressed as mean ± SD for 6 rabbits. No significant difference was found. CBF/MBR changes to baseline levels were shown in parentheses.

### 3.3. Effects of individuality and treatment

Randomized block ANOVA revealed that there were wide ranges of distribution of differences for the basal blood flow measurement and that animals' individuality had significant effects on MBR and CBF (Table 1). Distributions of differences for the time-course changes were relatively narrow. Although the time-course changes in MBR and CBF during ET-1 treatment were not significant, those during CO<sub>2</sub> treatment were significant by repeated measure analysis (Table 1).

Average and individual changes in CBF after treatments are shown in Tables 2 and 3 and Fig. 4, respectively. CBF had a tendency of increasing after CO<sub>2</sub> inhalation (CBF was increased in 6 cases out of 9). ET-1 administration decreased CBF in 5 cases out of 6 though the effect was not significant because CBF was markedly increased in just one case. Representative hydrogen density curve charts are shown in Fig. 5. Average changes in MBR after treatments are shown in Tables 2 and 3. Typical examples of 2-dimensional color-coded MBR maps are shown in Fig. 6.

## 4. Discussion

This report is the first to verify the correlation of MBR, a new index obtained by CCD-equipped LSFG, with CBF obtained by the hydrogen gas clearance method in the ONH. A significant and positive correlation between the absolute values of CBF and MBR at baseline, as well as their relative changes, was found in the current study. This result suggests that MBR may correlate with CBF and also change with CBF, as an index of blood flow in the ONH, linearly. Since a similar experiment cannot be performed in humans, the

present study provides important basal data for the measurement of MBR in humans, though these data cannot be applied directly to humans because of their many histophysiological differences with rabbits.

A power analysis (Correlation: point biserial model) by G\*Power software (v. 3.1.3) showed that total sample size of 9 is needed under the condition of effect size of 0.7, error probability ( $\alpha$ ) of 0.05 and power ( $1 - \beta$ ) of 0.8. Therefore, the sample sizes of 14 and 39 in the current study would be sufficient statistically.

In the present study, inhalation of CO<sub>2</sub> or intravenous administration of ET-1 altered CBF obtained by the hydrogen gas clearance method in rabbit ONH. These results are, at least partly, consistent with previous reports (Sugiyama et al., 1995, 1996). The relative values of CBF and MBR to the initial levels were in the range of 0.74–1.27 and 0.76–1.35, respectively. A significant and positive correlation was also found between the relative changes in CBF and MBR values induced by CO<sub>2</sub> inhalation and ET-1 injection. This correlation suggests that changes in MBR may indicate those in CBF in the ONH. These results appear similar to a previous report (Sugiyama et al., 1996). Though the  $r$  value in this study (0.67) was obviously different from that in the previous paper (0.92), the comparison of  $r$  values from different experiments does not seem fair since they can be affected by many factors.

In the current study, the  $r$  value for the correlation between the absolute values of MBR and CBF was 0.73; this was relatively large and comparable to that between the relative values during CO<sub>2</sub> inhalation and ET-1 injection. This result indicates quantifiability of absolute values of MBR at least under a certain condition. On the other hand, the randomized block ANOVA in the current study revealed significant effects of the individuality of animals on basal values of CBF and MBR. Therefore, care must be taken in interpreting absolute values across individuals, even though the absolute values of MBR were significantly correlated with CBF. In general, measurement results obtained with apparatus that employ lasers are affected by the degree of absorption or reflection of the laser beam in the specific tissue. Particularly in humans, careful interpretation is needed due to relatively large topographical or color differences of the ONH induced by individuality or diseases, which affect absorption and reflection. Actually, we have data on individual variation in MBRs of young normal volunteers; MBRs in the temporal rim were measured in the range of 6.3–13.8 (mean ± SD = 10.6 ± 2.5,  $n = 9$ ). In addition, MBRs in the nasal

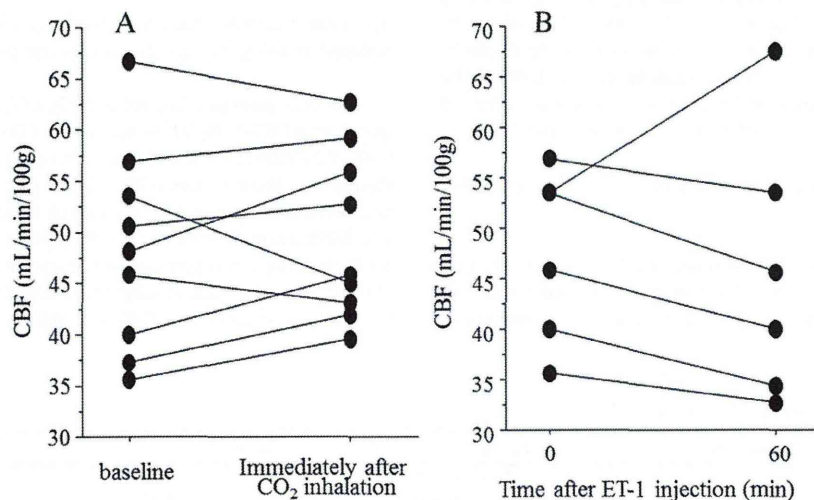


**Fig. 4.** Individual changes in CBF after 5-min inhalation of 10% CO<sub>2</sub> (A) and administration of 10<sup>-10</sup> mol/kg ET-1 (B). CBF was increased in 6 cases out of 9, and decreased in 5 cases out of 6 in A and B, respectively.

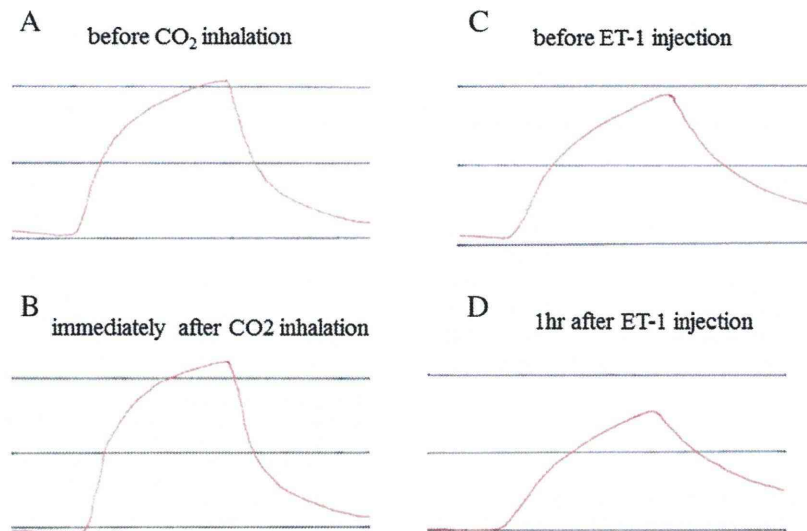


**Fig. 5.** Representative examples of the hydrogen gas clearance curve. A and B: before and immediately after 5-min inhalation of 10% CO<sub>2</sub> in the same rabbit (A is the same as Fig. 1A). CBF values were 65.3 and 77.6 mL/min/100 g, respectively. C and D: before and 1 h after administration of 10<sup>-10</sup> mol/kg ET-1 in another same rabbit. CBF values were 40.3 and 32.8 mL/min/100 g, respectively.

rim of them were measured as  $17.8 \pm 3.9$ , which are much different from those in the temporal rim. Therefore, the relatively wide range of ONH blood flow in the present study might be due to an individual difference as well as a regional difference.

As a problematic issue for the LSFG apparatus, the zero-offset for MBR was rather large (around 2.5) in the current study. We actually obtained 6.1 and 1.9 as mean values of MBR ( $n = 2$ ) at the same spot of ONH just before and shortly after a rabbit was euthanized (the

hydrogen gas clearance method cannot be available while it is dead because inhalation is impossible then) in the additional experiment. This result (mean value of MBR was 1.9 when blood flow was stopped in dead rabbits) is almost consistent with the zero-offset of approximately 2.5. In addition, since a range of baseline values of MBR was 3.5–6.0, the ratio of the highest to the lowest (6.0/3.5) was smaller than those by the hydrogen gas clearance method (83.5/32.4). Taken together, there seems to be a room for more

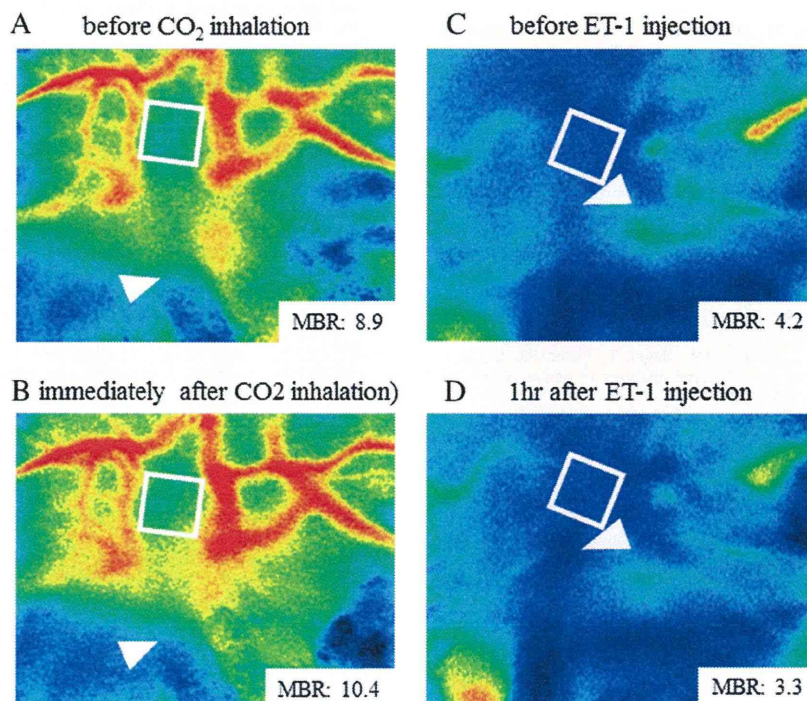


**Fig. 6.** Representative examples of color-coded MBR maps obtained by LSFG. A and B: before and immediately after 5-min inhalation of 10% CO<sub>2</sub> in the same rabbit. C and D: before and 1 h after administration of 10<sup>-10</sup> mol/kg ET-1 in another rabbit. Arrowheads indicate the tips of electrodes for the hydrogen gas clearance method, and white squares indicate the areas analyzed by LSFG.

adequate calibration of MBR values. While these results (a relatively large zero-offset and a smaller relative change in MBR) were only for the animal model in the current study. Further investigation using other animals should also be needed in the future for validation of quantifiability of measurement of ONH microcirculation by LSFG.

Many agents have been reported to alter ocular blood flow (Araie and Mayama, 2011; Shimazawa et al., 1999; Sugiyama and Azuma, 1995; Sugiyama et al., 2010, 2011; Tokushige et al., 2011; Waki et al., 2001). Since the present study revealed that MBR may correlate with tissue blood flow in the ONH, LSFG-NAVI™ will likely provide new relevant information concerning the ONH blood flow in glaucoma and support in verifying whether increasing ONH blood flow could be a promising strategy for glaucoma management.

## 5. Conclusions

Our results suggest that MBR obtained by CCD-equipped LSFG may correlate with CBF and also change with CBF, as an index of blood flow in the ONH, linearly.

## Financial disclosure

H. Takahashi and H. Tokushige are employees of Senju Pharmaceutical Co., Ltd. The other authors have no financial disclosures.

## Acknowledgments

The authors thank Y.T. for her technical support and kindest encouragement, Mr. Mitsunori Waki for his technical advice and valuable discussions, and Dr. Tomoyuki Wada for his advice concerning statistics and his encouragement.

## References

- Aizawa, N., Yokoyama, Y., Chiba, N., Omodaka, K., Yasuda, M., Otomo, T., Nakamura, M., Fuse, N., Nakazawa, T., 2011. Reproducibility of retinal circulation measurements obtained using laser speckle flowgraphy-NAVI in patients with glaucoma. *Clin. Ophthalmol.* 5, 1171–1176.
- Araie, M., Mayama, C., 2011. Use of calcium channel blockers for glaucoma. *Prog. Retin. Eye Res.* 30, 54–71.
- Aukland, K., Bower, B.F., Berliner, R.W., 1964. Measurement of local blood flow with hydrogen gas. *Circ. Res.* 14, 164–187.
- Caprioli, J., Coleman, A.L., 2010. Blood pressure, perfusion pressure, and glaucoma. *Am. J. Ophthalmol.* 149, 704–712.
- Csete, K., Vezekényi, Z., Dóczy, T., Papp, J.G., Bodosi, M., Barzó, P., 2004. Comparison of regional vasomotor responses to acetazolamide and CO<sub>2</sub> in rabbit cerebrum and cerebellum, measured by a hydrogen clearance method. *Acta Physiol. Scand.* 182, 287–294.
- Ernest, J.T., 1976. Optic disc blood flow. *Trans. Ophthalmol. Soc. U.K.* 96, 348–351.
- Garhofer, G., Bek, T., Boehm, A.G., Gherghel, D., Grunwald, J., Jeppesen, P., Kergoat, H., Kotliar, K., Lanzl, I., Lovasik, J.V., Nagel, E., Vilser, W., Orgul, S., Schmetterer, L., 2010. Use of the retinal vessel analyzer in ocular blood flow research. *Acta Ophthalmol.* 88, 717–722.
- Grieshaber, M.C., Mozaffarieh, M., Flammer, J., 2007. What is the link between vascular dysregulation and glaucoma? *Surv. Ophthalmol.* 52 (Suppl. 2), S144–S154.
- Harris, A., Kagemann, L., Ehrlich, R., Rospigliosi, C., Moore, D., Siesky, B., 2008a. Measuring and interpreting ocular blood flow and metabolism in glaucoma. *Can. J. Ophthalmol.* 43, 328–336.
- Harris, A., Werne, A., Cantor, L.B., 2008b. Vascular abnormalities in glaucoma: from population-based studies to the clinic? *Am. J. Ophthalmol.* 145, 595–597.
- Konishi, N., Tokimoto, Y., Kohra, K., Fujii, H., 2002. New laser speckle flowgraphy system using CCD camera. *Opt. Rev.* 9, 163–169.
- Logan, J.F., Rankin, S.J., Jackson, A.J., 2004. Retinal blood flow measurements and neuroretinal rim damage in glaucoma. *Br. J. Ophthalmol.* 88, 1049–1054.
- Moore, D., Harris, A., Wudunn, D., Kheradiya, N., Siesky, B., 2008. Dysfunctional regulation of ocular blood flow: a risk factor for glaucoma? *Clin. Ophthalmol.* 2, 849–861.
- Nagahara, M., Tamaki, Y., Araie, M., Fujii, H., 1999. Real-time blood velocity measurements in human retinal vein using the laser speckle phenomenon. *Jpn. J. Ophthalmol.* 43, 186–195.
- Pemp, B., Georgopoulos, M., Vass, C., Fuchsjäger-Mayrl, G., Luksch, A., Rainer, G., Schmetterer, L., 2009. Diurnal fluctuation of ocular blood flow parameters in patients with primary open-angle glaucoma and healthy subjects. *Br. J. Ophthalmol.* 93, 486–491.
- Riva, C.E., Geiser, M., Petrig, B.L., 2010. Ocular blood flow assessment using continuous laser doppler flowmetry. *Acta Ophthalmol.* 88, 622–629.
- Shimazawa, M., Sugiyama, T., Azuma, I., Araie, M., Iwakura, Y., Watari, M., Sakai, T., Hara, H., 1999. Effect of lomerizine, a new Ca<sup>2+</sup>-channel blocker, on the microcirculation in the optic nerve head in conscious rabbits: a study using a laser speckle technique. *Exp. Eye Res.* 69, 185–193.
- Srinivasan, V.J., Atochin, D.N., Radhakrishnan, H., Jiang, J.Y., Ruvinskaya, S., Wu, W., Barry, S., Cable, A.E., Ayata, C., Huang, P.L., Boas, D.A., 2011. Optical coherence tomography for the quantitative study of cerebrovascular physiology. *J. Cereb. Blood Flow Metab.* 31, 1339–1345.
- Stalmans, I., Vandewalle, E., Anderson, D.R., Costa, V.P., Frenkel, R.E., Garhofer, G., Grunwald, J., Gugleta, K., Harris, A., Hudson, C., Januleviciene, I., Kagemann, L., Kergoat, H., Lovasik, J.V., Lanzl, I., Martinez, A., Nguyen, Q.D., Plange, N., Reitsamer, H.A., Sehi, M., Siesky, B., Zeitz, O., Orgul, S., Schmetterer, L., 2011. Use of colour doppler imaging in ocular blood flow research. *Acta Ophthalmol.* 89, e609–630.
- Sugiyama, T., Araie, M., Riva, C.E., Schmetterer, L., Orgul, S., 2010. Use of laser speckle flowgraphy in ocular blood flow research. *Acta Ophthalmol.* 88, 723–729.
- Sugiyama, T., Azuma, I., 1995. Effect of UF-021 on optic nerve head circulation in rabbits. *Jpn. J. Ophthalmol.* 39, 124–129.
- Sugiyama, T., Moriya, S., Oku, H., Azuma, I., 1995. Association of endothelin-1 with normal tension glaucoma: clinical and fundamental studies. *Surv. Ophthalmol.* 39 (Suppl. 1), S49–S56.
- Sugiyama, T., Shibata, M., Kajiura, S., Okuno, T., Tonari, M., Oku, H., Ikeda, T., 2011. Effects of fasudil, a rho-associated protein kinase inhibitor, on optic nerve head blood flow in rabbits. *Invest. Ophthalmol. Vis. Sci.* 52, 64–69.
- Sugiyama, T., Utsumi, T., Azuma, I., Fujii, H., 1996. Measurement of optic nerve head circulation: comparison of laser speckle and hydrogen clearance methods. *Jpn. J. Ophthalmol.* 40, 339–343.
- Takayama, J., Tomidokoro, A., Ishii, K., Tamaki, Y., Fukaya, Y., Hosokawa, T., Araie, M., 2003. Time course of the change in optic nerve head circulation after an acute increase in intraocular pressure. *Invest. Ophthalmol. Vis. Sci.* 44, 3977–3985.
- Tamaki, Y., Araie, M., Fukaya, Y., Nagahara, M., Imamura, A., Honda, M., Obata, R., Tomita, K., 2003. Effects of lomerizine, a calcium channel antagonist, on retinal and optic nerve head circulation in rabbits and humans. *Invest. Ophthalmol. Vis. Sci.* 44, 4864–4871.
- Tamaki, Y., Araie, M., Kawamoto, E., Eguchi, S., Fujii, H., 1995. Non-contact, two-dimensional measurement of tissue circulation in choroid and optic nerve head using laser speckle phenomenon. *Exp. Eye Res.* 60, 373–383.
- Tamaki, Y., Araie, M., Kawamoto, E., Eguchi, S., Fujii, H., 1994. Noncontact, two-dimensional measurement of retinal microcirculation using laser speckle phenomenon. *Invest. Ophthalmol. Vis. Sci.* 35, 3825–3834.
- Tamaki, Y., Araie, M., Tomita, K., Tomidokoro, A., 1996. Time change of nicardipine effect on choroidal circulation in rabbit eyes. *Curr. Eye Res.* 15, 543–548.
- Tokushige, H., Waki, M., Takayama, Y., Tanihara, H., 2011. Effects of Y-39983, a selective rho-associated protein kinase inhibitor, on blood flow in optic nerve head in rabbits and axonal regeneration of retinal ganglion cells in rats. *Curr. Eye Res.* 36, 964–970.
- Tomidokoro, A., Araie, M., Tamaki, Y., Tomita, K., 1998. In vivo measurement of iridial circulation using laser speckle phenomenon. *Invest. Ophthalmol. Vis. Sci.* 39, 364–371.
- Tomita, K., Araie, M., Tamaki, Y., Nagahara, M., Sugiyama, T., 1999. Effects of nilvadipine, a calcium antagonist, on rabbit ocular circulation and optic nerve head circulation in NTG subjects. *Invest. Ophthalmol. Vis. Sci.* 40, 1144–1151.
- Waki, M., Sugiyama, T., Watanabe, N., Ogawa, T., Shirahase, H., Azuma, I., 2001. Effect of topically applied igandipine dihydrochloride, a novel calcium antagonist, on optic nerve head circulation in rabbits. *Jpn. J. Ophthalmol.* 45, 76–83.
- Watanabe, G., Fujii, H., Kishi, S., 2008. Imaging of choroidal hemodynamics in eyes with polypoidal choroidal vasculopathy using laser speckle phenomenon. *Jpn. J. Ophthalmol.* 52, 175–181.
- Yamazaki, Y., Drance, S.M., 1997. The relationship between progression of visual field defects and retrobulbar circulation in patients with glaucoma. *Am. J. Ophthalmol.* 124, 287–295.



ORIGINAL ARTICLE

## The Influence of Posture Change on Ocular Blood Flow in Normal Subjects, Measured by Laser Speckle Flowgraphy

Yukihiro Shiga<sup>1</sup>, Masahiko Shimura<sup>2</sup>, Toshifumi Asano<sup>1</sup>, Satoru Tsuda<sup>1</sup>, Yu Yokoyama<sup>1</sup>, Naoko Aizawa<sup>1</sup>, Kazuko Omodaka<sup>1</sup>, Morin Ryu<sup>1</sup>, Shunji Yokokura<sup>1</sup>, Takayuki Takeshita<sup>1</sup> and Toru Nakazawa<sup>1</sup>

<sup>1</sup>Department of Ophthalmology, Tohoku University Graduate School of Medicine, Miyagi, Japan and  
<sup>2</sup>Department of Ophthalmology, NTT East Japan Tohoku Hospital, Sendai, Japan

### ABSTRACT

**Purpose:** To investigate, using laser speckle flowgraphy (LSFG), the autoregulation of ocular blood flow (BF) in response to posture change.

**Methods:** This study comprised 20 healthy volunteers (mean age  $30.0 \pm 8.5$ ). The mean blur rate (MBR) of the ocular circulation in the subjects was assessed in both a sitting and a supine position every 2 min over the course of 10 min. Baseline measurements of the MBR at the optic nerve head (ONH) and the choroid were taken in a sitting position. Increases in the MBR ratio in a supine position were calculated with reference to this baseline. Intraocular pressure (IOP), systemic blood pressure and heart rate in the brachial artery were also recorded.

**Results:** In the ONH, the MBR ratio increased significantly over the baseline after 2 min ( $104.8 \pm 5.0\%$ ,  $p = 0.001$ ) and 4 min ( $104.4 \pm 5.6\%$ ,  $p = 0.005$ ), in a supine position, but decreased to the initial level after only 6 min. In the choroid, on the other hand, while the MBR ratio also increased significantly after 2 min in a supine position ( $113.7 \pm 8.1\%$ ,  $p < 0.001$ ), it kept this significant increase over the time course of 10 min. After 10 min in a supine position, IOP increased significantly ( $p < 0.001$ ), systolic blood pressure decreased significantly ( $p < 0.001$ ), but diastolic blood pressure did not change significantly compared to the baseline. ( $p = 0.07$ )

**Conclusions:** ONH and choroidal circulation have significantly different hemodynamics in response to posture change in healthy volunteers. This finding suggests that LSFG enables us to assess the autoregulation of BF in the ONH.

**Keywords:** Autoregulation, choroid, laser speckle flowgraphy, ocular blood flow, optic nerve head

### INTRODUCTION

The regulation of blood flow (BF) in response to posture change is important to ensure an adequate supply of oxygen and nutrients to all tissues in the body. Changes in posture create changes in ocular perfusion pressure (OPP) induced by gravity. Therefore, the local microvasculature of ocular structures has to compensate for the altered OPP and altered metabolic stimuli.

Recent studies have investigated the influence of posture change on choroidal BF (ChBF) in normal subjects by using laser doppler flowmetry (LDF).<sup>1,2</sup> Their results have suggested a linear relationship between subfoveal ChBF and OPP, indicating that the vascular bed responds passively to increases in OPP.

The response of retinal and optic nerve head (ONH) circulation to posture change in normal subjects has also been studied with a variety of techniques.<sup>3–7</sup> An autoregulatory response in retinal

Received 10 September 2012; revised 17 November 2012; accepted 10 December 2012; published online 6 May 2013

Correspondence: Toru Nakazawa, MD, PhD, Department of Ophthalmology, Tohoku University Graduate School of Medicine, 1-1, Seiryō, Aoba, Sendai Miyagi: 980-8574, Japan. Tel: +81-22-717-7294. Fax: +81-22-717-7298. E-mail: ntoru@oph.med.tohoku.ac.jp

and ONH BF seems to occur despite variations in OPP. Due to technical limitations, however, conventional instruments have only a small capture area, making it hard to simultaneously obtain images and evaluate differing hemodynamics in the ONH, retinal vessels and choroidal circulation.

Laser speckle flowgraphy (LSFG), by contrast, allows us to make the necessary simultaneous quantification of microcirculation in the ONH, the choroid at the fovea, and the retinal vessels. It is a non-contact technique based on the laser speckle phenomenon, and has been shown to be reliable and reproducible.<sup>8,9</sup> Most importantly, LSFG takes just a few seconds to acquire an image of ocular circulation, and it can be used in living eyes.<sup>8</sup> This quick acquisition of images enables researchers to measure dynamic changes in ONH BF and ChBF during posture change over a shorter period.

This study used LSFG to simultaneously examine dynamic changes in ONH BF and ChBF in normal subjects during the change from a sitting to a supine position, and used the resulting data to compare vascular autoregulation in these two regions.

## MATERIALS AND METHODS

### Subjects

This study comprised twenty healthy, non-smoking subjects (age:  $30.0 \pm 8.5$  years old, male: female = 15:5), recruited from volunteers at Tohoku University Hospital, Miyagi, Japan. All subjects included in this study had baseline intraocular pressure (IOP) in both eyes below 22 mmHg, as measured by Goldmann applanation tonometry, and normal findings on a slit lamp or funduscopic examination, as well as refractive error within a range of  $-8.75$  to  $+0.25$  diopter (mean:  $-3.10 \pm 2.83$ ), and pupillary diameters measurable by LSFG-NAVI without mydriasis. Subjects were excluded if they had a history of ophthalmic or general disorders, ocular laser or incisional surgery in either eye, or systemic or topical medication. All subjects abstained from alcohol and caffeine for at least six hours before the measurements.

This study monitored only the left eyes of each participant. The local ethics committee approved the procedures and followed the tenets of the Declaration of Helsinki. All participants gave their informed consent before starting the study.

### Measurement of Clinical Parameters

Both systemic blood pressure and heart rate (HR) were appropriately measured in the left brachial artery at the height of the heart by an automated blood pressure monitor (HEM-759 E,

Omron Corporation, Kyoto, Japan). Mean arterial pressure (MAP) was calculated from systolic blood pressure (sBP) and diastolic blood pressure (dBP) according to the formula:  $MAP = dBP + 0.42(sBP - dBP)$ .<sup>1,2,10</sup>

Baseline IOP was determined using Goldmann applanation tonometry, with subjects in a sitting position. IOP in a supine position was measured with a handheld tonometer (Tonopen; Mentor, Norwell, MA).

OPP in a sitting position was calculated according to the formula:  $OPP_{sitting} = 2/3 MAP_{sitting} - IOP$ , which accounts for the drop in blood pressure between the brachial and ophthalmic artery when the subject is sitting.<sup>11</sup> The OPP in a supine position was calculated from following equation:  $OPP_{supine} = MAP_{supine} - IOP$ .<sup>4</sup> Since preliminary experiments on five healthy volunteers had shown that there was no significant IOP difference after 2 or 10 min in a supine position ( $14.8 \pm 1.6$ ,  $15.4 \pm 1.7$  mmHg, respectively,  $p = 0.55$ ), and to avoid the influence of anesthesia on the ocular circulation, IOP was not recorded during the 2 min measurements taken in a supine position over the course of 10 min. IOP for the supine position was measured after the full 10 min, and this measurement was substituted for the 2 min measurements when  $OPP_{supine}$  was calculated.

### LSFG

We assessed ocular circulation BF using the MBR, which we measured using a newer, non-invasive version of LSFG (LSFG-NAVI Software, Iizuka, Japan). This instrument consists of a fundus camera equipped with a diode laser (wavelength 830 nm), and an ordinary charge-coupled device (CCD) camera ( $750$  (width)  $\times$   $360$  (height) pixels). The mechanism of LSFG has been described in detail elsewhere.<sup>12,13</sup> MBR was determined using the pattern of speckle contrast produced by the interference of a laser scattered by blood cells moving in the ocular fundus. This is known to be closely associated with BF velocity.<sup>14</sup> The relative velocity of BF can be derived from the inverse of speckle contrast values using computationally intensive calculations.<sup>15</sup> We determined the MBR ratio by normalizing the values measured in a supine position to the baseline (measured in a sitting position) for each subject. The device acquired images of the BF map continuously at the rate of 30 images per second. We analyzed the data from a 5 s time period.<sup>8</sup>

A composite map of BF was obtained at the ONH and the fovea, and the equipped software automatically calculated the MBR in arbitrary units (au) for each area (Figure 1). As depicted in Figure 1, the MBR in the ONH included measurements for the large vessel and capillary areas. This study examined only the

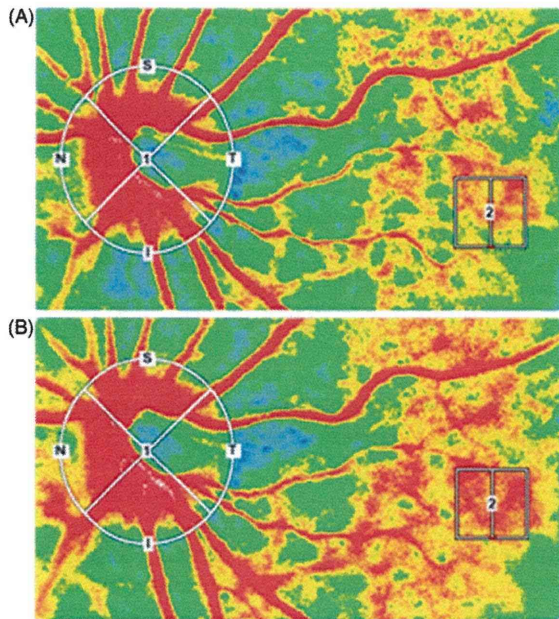


FIGURE 1. Representative retinal images of ocular BF, taken using LSFG, in a sitting position (A) and after 6 min in a supine position (B). The color-coded areas around the ONH (white circle #1) and on the fovea (white square #2) are automatically tracked in the images at each time point.

MBR in the large vessel area of the ONH. The MBR in the fovea was obtained from an area within the fovea one disc diameter in size (150 × 150 pixels).<sup>9,16</sup> As shown in Figure 2, we used a raised platform specially designed for the safety of the subjects to measure the MBR in a supine position.

**Experimental Protocols**

**Validity Assessment of LSFG-NAVI in the Supine Position**

To assess the validity of LSFG-NAVI measurements in the supine position, we compared variations between the MBR and velocity in both the sitting and supine positions. Figure 3 shows the schematic view of the experimental set up with the LSFG-NAVI system. Following a previous study,<sup>17</sup> the rotating opal glass plate (OGP) was placed in front of the LSFG-NAVI system’s objective lens (Le), and its movement speed was assumed to be the change in BF velocity. The MBR was obtained by changing the speed of the OGP for each position, and then evaluating whether there were any significant differences in the regression equations of the variation between the MBR and the velocity of the OGP.

**Reproducibility Assessment of LSFG-NAVI in the Supine Position**

To assess the intrasession reproducibility of LSFG-NAVI measurements in the supine position, we

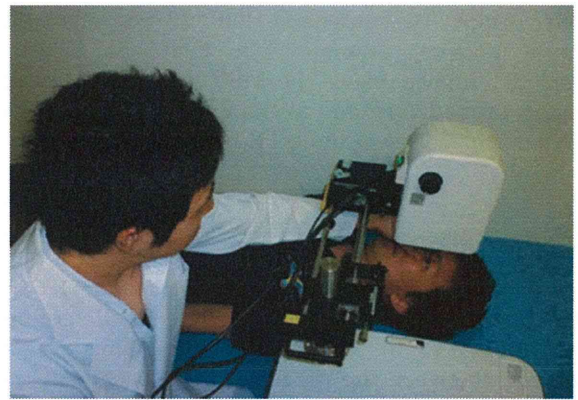


FIGURE 2. A raised platform specially designed in the consideration of patients’ safety was used to measure the MBR in the supine position.

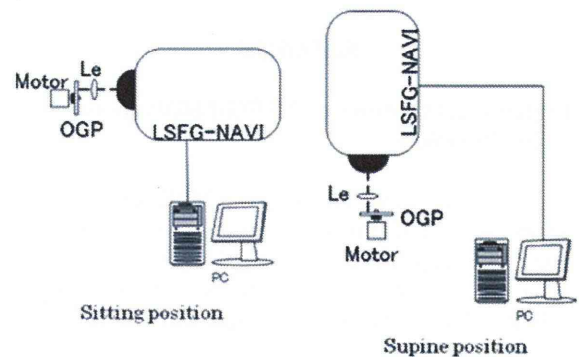


FIGURE 3. Schematic view of the experimental set up for the evaluation of the LSFG-NAVI system’s validity. A rotating opal glass (OGP) is located in front of the lens (Le).

performed a preliminary experiment on ten healthy subjects (20 eyes, mean age: 27.9 ± 5.7 years old; male: female = 5:5). Two parameters indicating reproducibility, the coefficient of variation (COV) and intraclass correlation coefficient (ICC), were evaluated with MBR measurements obtained using LSFG-NAVI during three continuous examinations, on the same day, after 10 min in a supine position.

**Testing Protocol**

On the day of the test, following a slit lamp examination, a fundoscopic examination and baseline IOP measurement taken with Goldmann applanation tonometry, each subject was asked to sit in an upright position for 10 min in a dark room before further investigation. SBP, dBP and HR were then recorded, and the MBR was assessed in a sitting position, to be used as the baseline measurement. Soon after, the subject was asked to lie down on a bed, and sBP, dBP and HR were recorded just before an LSFG measurement was taken, this was repeated every 2 min for the

next 10 min. We measured IOP 10 min after the supine position. Alterations in ONH BF velocity were determined using the MBR ratio in the large vessels of the ONH, and alterations in ChBF velocity were evaluated using the MBR ratio at the fovea.

### Statistics

All data are shown as mean  $\pm$  standard deviation. We used an analysis of covariance to determine any differences in the regression equations of the variation between the MBR and the velocity of the OGP for the sitting and supine positions. Wilcoxon signed-rank tests were applied to assess differences in the measurements for different body positions. The significance level was set at  $p < 0.05$ .

## RESULTS

### Validity Assessment of LSF-G-NAVI in the Supine Position

Figure 4(A) shows variation in the MBR relative to the velocity of the OGP, in the sitting position. The MBR value increases linearly with increasing velocity. Figure 4(B) shows similar results from the supine position. There were no significant differences

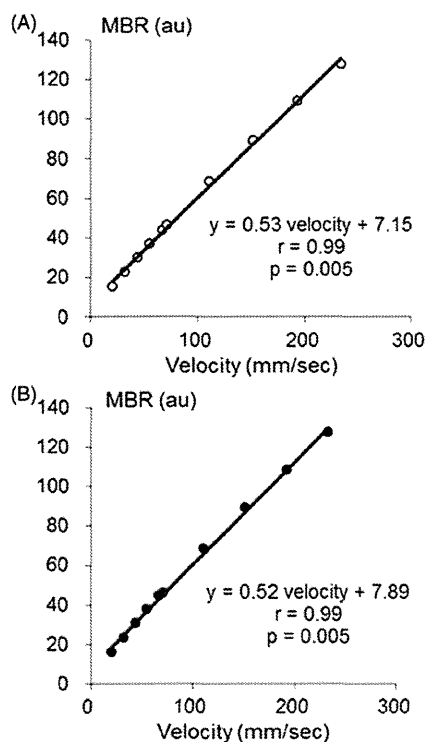


FIGURE 4. The variation in MBR against the velocity of the OGP in the sitting (A) and supine (B) positions.

between the regression equations for each position ( $p = 0.60$ ).

### Reproducibility of LSF-G-NAVI in the Supine Position

Reproducibility of LSF-G-NAVI was similar in the large vessel area of the ONH and the choroid (large vessel area: COV:  $6.72 \pm 5.11\%$ , ICC: 0.90; choroid: COV:  $7.46 \pm 5.81\%$ , ICC: 0.95).

### Alteration of Systemic Blood Pressure in Response to Posture Change

In a sitting position, sBP and dBP were  $124.9 \pm 11.2$  mmHg and  $76.1 \pm 15.0$  mmHg, respectively. After the posture change to a supine position, both sBP and dBP did not alter for 2 min. After that, sBP gradually decreased and was statistically significantly lower than the initial sBP (in a sitting position). There was a significant decrease in dBP at four and 6 min after the posture change, after which it returned to the initial level (Figure 5A). The time course of MAP was calculated from sBP and dBP and is depicted in Figure 5(B). The alteration in MAP after the posture change was similar to that in sBP.

### Alteration of IOP and OPP in Response to Posture Change

In a sitting position, IOP was  $13.4 \pm 2.3$  mmHg. IOP in a supine position increased significantly to  $16.3 \pm 2.5$  mmHg after 10 min (Figure 5C). The time course for OPP was calculated from MAP and IOP, and is depicted in Figure 5(D). In a sitting position, OPP was  $51.0 \pm 7.1$  mmHg. Two minutes after the posture change, OPP first increased significantly, to  $78.5 \pm 11.6$  mmHg, and then gradually decreased. After 10 min, it was still higher than the baseline, at  $74.8 \pm 9.8$  mmHg.

### Alteration of MBR in Response to Posture Change

In a sitting position, the MBR in the vessel area of the ONH was  $45.4 \pm 7.3$  au. The MBR ratio was defined as 100% in each subject. After the posture change, the MBR ratio in the vessel area of the ONH gradually rose, reaching  $104.4 \pm 5.6\%$  at 4 min, a significant increase, but soon decreased to the initial level, after 6 min (Figure 6A). The MBR in the choroid was  $12.2 \pm 4.0$  au. Two minutes after the posture change, the MBR ratio suddenly rose to  $113.7 \pm 8.1\%$ , and

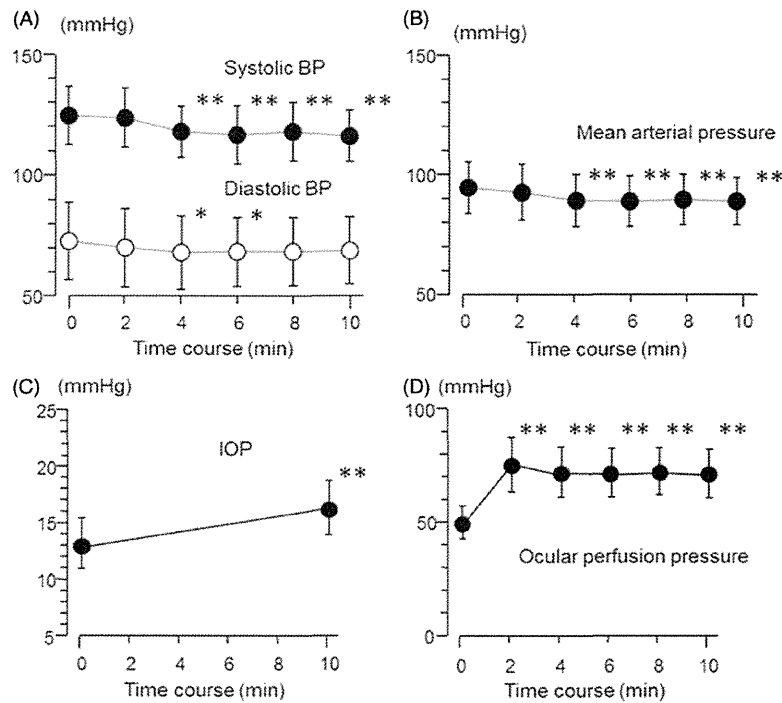


FIGURE 5. Dynamic changes in systolic (●) and diastolic (○) blood pressure in response to a change in posture from a sitting (0 min) to supine position (A). Dynamic changes in MAP (B), IOP (C), and OPP (D) are also depicted. The asterisk indicates a statistically significant difference from the initial sitting position. (Wilcoxon signed-rank tests. \*:  $p < 0.05$ . \*\*:  $p < 0.01$ ).

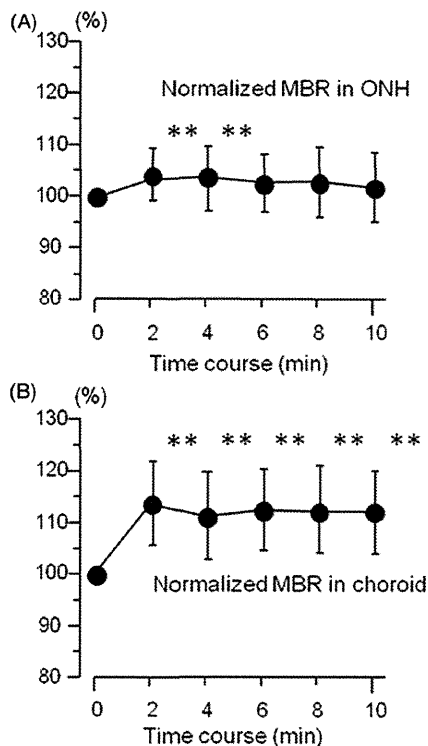


FIGURE 6. The dynamic change in MBR, normalized to the initial sitting position, at the ONH (A) and on the fovea (B) after a posture change to a supine position. The asterisk indicates a statistically significant difference from the initial sitting position. (Wilcoxon signed-rank tests. \*:  $p < 0.05$ . \*\*:  $p < 0.01$ ).

stayed at this significantly increased level for the entire time course of 10 min (Figure 6B).

### DISCUSSION

The authors first evaluated the validity and reproducibility of LSFG-NAVI in the supine position. Variation in the MBR was found to have a linear relationship with the velocity of the OGP in various positions. This result is consistent with previous research.<sup>17</sup> In addition to the validity assessment, we also tested the reproducibility of LSFG-NAVI in the supine position. Our group has previously reported on the reproducibility of determining MBR using LSFG-NAVI in the sitting position in patients with glaucoma or preperimetric glaucoma (COV:  $1.9 \pm 1.1$ – $12.4 \pm 12.4\%$ ; ICC: 0.82–0.98).<sup>9</sup> Results from this regarding the reproducibility of MBR in the supine position are similar to the previous research. As mentioned above, LSFG shows favorable reproducibility in the vessel area of the ONH and choroid in both the supine and sitting positions. This suggests that this instrument is suitable for monitoring changes in ocular circulation in response to posture change.

The major finding of this study is that the dynamic change in BF velocity after posture change, as measured by LSFG-NAVI, differs between the large vessel area of the ONH and the choroidal vessels in normal subjects. Posture change caused a prompt

and continuous increase in OPP for 10 min. In the ONH, a slight increase in BF velocity after posture change was observed within 4 min and was corrected within 6 min.

The large vessel area of the ONH, which we measured with LSFG-NAVI, is thought to be composed mainly of retinal arterial and venous circulation, but LSFG cannot measure retinal and choroidal circulation separately due to technical limitations.<sup>8</sup>

The finding that ONH BF velocity increases significantly after 2 min indicates that it compensates for retinal vessel responses to posture change.

Several studies of regulation in the retinal vasculature in response to isometric exercise and posture change have suggested that an increase in systemic blood pressure or retinal perfusion pressure induces a vasoconstrictive response in the retinal arterioles.<sup>3,18–20</sup> Baer and Hill<sup>5</sup> have reported that the caliber of the retinal arteries decreased significantly, with a corresponding increase in the caliber of the retinal veins, approximately 90 s after tilting the head to a bowed position. That reports tends to support the premise of this author.

The finding that velocity in the ONH returned to the initial level after only 6 min, despite a continuous increase in OPP, indicates the existence of an autoregulatory mechanism that begins working within several minutes.

Generally, there are thought to be both myogenic and metabolic components to the mechanism of retinal BF autoregulation.<sup>21</sup> The myogenic component is defined as the response of the vascular smooth muscle and endothelial cells to mechanical forces, and this response may require several minutes to induce stable vessel diameters following an acute change in intravascular pressure.<sup>22,23</sup> By contrast, the metabolic component is the interaction of factors released from neurons and glial cells, which affects vascular smooth muscle cells and pericytes and changes the tone of vascular resistance. This response seems to occur within a few seconds.<sup>24</sup> Our results showed that the autoregulatory mechanism for ONH BF was complete after 6 min, meaning that our results for dynamic change possibly reflect the myogenic mechanism.

Ocular BF depends on the interaction of various factors, such as the vascular resistance generated by the diameter and length of the vessels, and blood viscosity. In this study, changes in these factors due to posture change were not measured due to the technical difficulty involved, but in the future, a simultaneous evaluation of OPP and these factors should be done to assess the driving force of BF.

In this study, the authors also measured the MBR in the choroid at the fovea, which is thought to reflect over 90% of the ChBF.<sup>13</sup> In the choroid, a significant increase in BF velocity was observed within 2 min, and was sustained for 10 min. This was synchronized with OPP dynamics. Since choroidal circulation is

mainly controlled by sympathetic innervation and is not autoregulated,<sup>25</sup> it has been believed that ChBF responds passively to changes in OPP.<sup>1,2</sup> Our finding of an approximately 14% increase in the MBR ratio in the choroid is similar to the 11% increase in ChBF reported by Longo<sup>1</sup>, although the two investigations differ in that our study used LSFG and focused on the period between 2 and 10 min after posture change, and the latter study used LDF and focused on the 2 min period after posture change. In this study, as in previous studies, dynamic change in the choroid correlated with OPP, suggesting a lack of autoregulation.

According to recent studies of retinal and ChBF, there is considerable evidence that vascular dysregulation in eyes with glaucoma<sup>26–29</sup> or diabetic retinopathy<sup>30</sup> occurs in the subclinical stages of these diseases. Recent studies have demonstrated that LSFG enables us to assess alterations in the autoregulation of ONH BF in experimental animals.<sup>31,32</sup> To the best of our knowledge, however, no information has yet been available on the use of LSFG-NAVI in human beings to assess changes in ocular circulation in response to posture change. The authors can confirm that this new approach for evaluating hemodynamics in ONH BF and ChBF in response to posture change using LSFG-NAVI may be useful in screening for certain eye diseases, due to its quick and easy acquisition of wide angle images of the retina. Our data accords with previous studies reporting that IOP increases significantly with a postural change from a sitting to a supine position,<sup>33,34</sup> Furthermore, the magnitude of the IOP elevation was higher in patients with glaucoma than in controls, which may indicate an association with glaucomatous damage.<sup>35–37</sup> Therefore, both vascular dysregulation and IOP change may be associated with the development and progression of glaucomatous change. Of course, we acknowledge the limitations of this study, which had only a small number of normal subjects. In the future, larger, multi-center studies using subjects with eye disease, particularly those with glaucoma, must be performed.

In conclusion, LSFG-NAVI showed favorable validity and reproducibility in both the supine position and the sitting position, suggesting that this instrument is suitable for monitoring changes in ocular circulation in response to posture change. Additionally, we investigated the dynamic response of ONH BF and ChBF to posture change in an intermediate time frame (2–10 min) of the vasculature's adaptation, allowing us to obtain similar results to previous studies.

## ACKNOWLEDGEMENTS

The authors thank Tim Hilts for reviewing the manuscript.

## DECLARATION OF INTEREST

There is no financial support to report, and there were no conflicts of interest in this study.

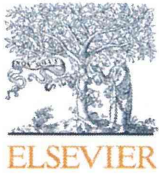
## REFERENCES

1. Longo A, Geiser MH, Riva CE. Posture changes and subfoveal choroidal blood flow. *Invest Ophthalmol Vis Sci* 2004;45:546–551.
2. Kaeser P, Orgul S, Zawinka C, Reinhard G, Flammer J. Influence of change in body position on choroidal blood flow in normal subjects. *Br J Ophthalmol* 2005;89:1302–1305.
3. Tachibana H, Gotoh F, Ishikawa Y. Retinal vascular autoregulation in normal subjects. *Stroke* 1982;13:149–155.
4. Hague S, Hill DW. Postural changes in perfusion pressure and retinal arteriolar calibre. *Br J Ophthalmol* 1988;72:253–257.
5. Baer RM, Hill DW. Retinal vessel responses to passive tilting. *Eye (Lond)* 1990;4:751–756.
6. Baxter GM, Williamson TH, McKillop G, Dutton GN. Color Doppler ultrasound of orbital and optic nerve blood flow: effects of posture and timolol 0.5%. *Invest Ophthalmol Vis Sci* 1992;33:604–610.
7. Feke GT, Pasquale LR. Retinal blood flow response to posture change in glaucoma patients compared with healthy subjects. *Ophthalmology* 2008;115:246–252.
8. Sugiyama T, Araie M, Riva CE, Schmetterer L, Orgul S. Use of laser speckle flowgraphy in ocular blood flow research. *Acta Ophthalmol* 2010;88:723–729.
9. Aizawa N, Yokoyama Y, Chiba N, Omodaka K, Yasuda M, Otomo T, et al. Reproducibility of retinal circulation measurements obtained using laser speckle flowgraphy-NAVI in patients with glaucoma. *Clin Ophthalmol* 2011;5:1171–1176.
10. Sayegh FN, Weigelin E. Functional ophthalmodynamometry. Comparison between brachial and ophthalmic blood pressure in sitting and supine position. *Angiology* 1983;34:176–182.
11. Riva CE, Grunwald JE, Petrig BL. Autoregulation of human retinal blood flow. An investigation with laser Doppler velocimetry. *Invest Ophthalmol Vis Sci* 1986;27:1706–1712.
12. Tamaki Y, Araie M, Kawamoto E, Eguchi S, Fujii H. Non-contact, two-dimensional measurement of tissue circulation in choroid and optic nerve head using laser speckle phenomenon. *Exp Eye Res* 1995;60:373–383.
13. Isono H, Kishi S, Kimura Y, Hagiwara N, Konishi N, Fujii H. Observation of choroidal circulation using index of erythrocytic velocity. *Arch Ophthalmol* 2003;121:225–231.
14. Fujii H, Nohira K, Yamamoto Y, Ikawa H, Ohura T. Evaluation of blood flow by laser speckle image sensing. Part 1. *Appl Opt* 1987;26:5321–5325.
15. Briers JD, Fercher AF. Retinal blood-flow visualization by means of laser speckle photography. *Invest Ophthalmol Vis Sci* 1982;22:255–259.
16. Tamaki Y, Araie M, Tomita K, Nagahara M, Tomidokoro A, Fujii H. Real-time measurement of human optic nerve head and choroid circulation, using the laser speckle phenomenon. *Jpn J Ophthalmol* 1997;41:49–54.
17. Konishi NTY, Kohra K, Fujii H. New laser speckle flowgraphy system using CCD camera. *Opt Rev* 2002;9:163–169.
18. Blum M, Bachmann K, Wintzer D, Riemer T, Vilser W, Strobel J. Noninvasive measurement of the Bayliss effect in retinal autoregulation. *Graefes Arch Clin Exp Ophthalmol* 1999;237:296–300.
19. Nagel E, Vilser W. Autoregulative behavior of retinal arteries and veins during changes of perfusion pressure: a clinical study. *Graefes Arch Clin Exp Ophthalmol* 2004;242:13–17.
20. Jeppesen P, Gregersen PA, Bek T. The age-dependent decrease in the myogenic response of retinal arterioles as studied with the Retinal Vessel Analyzer. *Graefes Arch Clin Exp Ophthalmol* 2004;242:914–919.
21. Pournaras CJ, Rungger-Brandle E, Riva CE, Hardarson SH, Stefansson E. Regulation of retinal blood flow in health and disease. *Prog Retin Eye Res* 2008;27:284–330.
22. Halpern W, Osol G. Influence of transmural pressure of myogenic responses of isolated cerebral arteries of the rat. *Ann Biomed Eng* 1985;13:287–293.
23. Rajagopalan S, Dube S, Canty Jr JM. Regulation of coronary diameter by myogenic mechanisms in arterial microvessels greater than 100 microns in diameter. *Am J Physiol* 1995;268:H788–H793.
24. Florence G, Seylaz J. Rapid autoregulation of cerebral blood flow: a laser-Doppler flowmetry study. *J Cereb Blood Flow Metab* 1992;12:674–680.
25. Delaey C, Van De Voorde J. Regulatory mechanisms in the retinal and choroidal circulation. *Ophthalmic Res* 2000;32:249–256.
26. Evans DW, Harris A, Garrett M, Chung HS, Kagemann L. Glaucoma patients demonstrate faulty autoregulation of ocular blood flow during posture change. *Br J Ophthalmol* 1999;83:809–813.
27. Fuchsjager-Mayrl G, Wally B, Georgopoulos M, Rainer G, Kircher K, Buehl W, et al. Ocular blood flow and systemic blood pressure in patients with primary open-angle glaucoma and ocular hypertension. *Invest Ophthalmol Vis Sci* 2004;45:834–839.
28. Galambos P, Vafiadis J, Vilchez SE, Wagenfeld L, Matthiessen ET, Richard G, et al. Compromised autoregulatory control of ocular hemodynamics in glaucoma patients after postural change. *Ophthalmology* 2006;113:1832–1836.
29. Ulrich A, Ulrich C, Barth T, Ulrich WD. Detection of disturbed autoregulation of the peripapillary choroid in primary open angle glaucoma. *Ophthalmic Surg Lasers* 1996;27:746–757.
30. Burgansky-Eliash Z, Nelson DA, Bar-Tal OP, Lowenstein A, Grinvald A, Barak A. Reduced retinal blood flow velocity in diabetic retinopathy. *Retina* 2010;30:765–773.
31. Liang Y, Downs JC, Fortune B, Cull G, Cioffi GA, Wang L. Impact of systemic blood pressure on the relationship between intraocular pressure and blood flow in the optic nerve head of nonhuman primates. *Invest Ophthalmol Vis Sci* 2009;50:2154–2160.
32. Shibata M, Oku H, Sugiyama T, Kobayashi T, Tsujimoto M, Okuno T, et al. Disruption of gap junctions may be involved in impairment of autoregulation in optic nerve head blood flow of diabetic rabbits. *Invest Ophthalmol Vis Sci* 2011;52:2153–2159.
33. Anderson DR, Grant WM. The influence of position on intraocular pressure. *Invest Ophthalmol* 1973;12:204–212.
34. Tsukahara S, Sasaki T. Postural change of IOP in normal persons and in patients with primary wide open-angle glaucoma and low-tension glaucoma. *Br J Ophthalmol* 1984;68:389–392.
35. Kiuchi T, Motoyama Y, Oshika T. Relationship of progression of visual field damage to postural changes

- in intraocular pressure in patients with normal-tension glaucoma. *Ophthalmology*. 2006;113:2150–2155.
36. Kiuchi T, Motoyama Y, Oshika T. Postural response of intraocular pressure and visual field damage in patients with untreated normal-tension glaucoma. *J Glaucoma* 2010;19:191–193.
37. Mizokami J, Yamada Y, Negi A, Nakamura M. Postural changes in intraocular pressure are associated with asymmetrical retinal nerve fiber thinning in treated patients with primary open-angle glaucoma. *Graefes Arch Clin Exp Ophthalmol* 2011;249: 879–885.

For personal use only.





## Molecular genetic analysis of primary open-angle glaucoma, normal tension glaucoma, and developmental glaucoma for the VAV2 and VAV3 gene variants in Japanese subjects

Dong Shi <sup>a,b,\*</sup>, Yoshimasa Takano <sup>b</sup>, Toru Nakazawa <sup>b</sup>, MinGe Mengkegale <sup>b</sup>, Shunji Yokokura <sup>b</sup>, Kohji Nishida <sup>b,c</sup>, Nobuo Fuse <sup>b,d</sup>

<sup>a</sup> Department of Ophthalmology, The Fourth Affiliated Hospital, China Medical University, 11 Xinhua Road, Heping District, Shenyang, Liaoning 110005, China

<sup>b</sup> Department of Ophthalmology, Tohoku University Graduate School of Medicine, 1-1 Seiryō-machi, Aoba-ku, Sendai, Miyagi 980-8574, Japan

<sup>c</sup> Department of Ophthalmology, Osaka University Graduate School of Medicine, Suita, Osaka 565-0871, Japan

<sup>d</sup> Department of Integrative Genomics, Tohoku Medical Megabank Organization, 1-1 Seiryō-machi, Aoba-ku, Sendai, Miyagi 980-8574, Japan

### ARTICLE INFO

#### Article history:

Received 26 January 2013

Available online 10 February 2013

#### Keywords:

POAG

NTG

DG

VAV2

VAV3

Gene screening

### ABSTRACT

The VAV2 and VAV3 genes have been implicated as being causative for primary open angle glaucoma (POAG) in the Japanese. We studied 168 unrelated Japanese patients with primary open-angle glaucoma (POAG), 163 unrelated Japanese patients with normal tension glaucoma (NTG), 45 unrelated Japanese patients with developmental glaucoma (DG), and 180 ethnically matched normal controls, to determine whether variants in the vav 2 guanine nucleotide exchange factor (VAV2) and vav 3 guanine nucleotide exchange factor (VAV3) genes are associated with POAG, NTG, or DG in the Japanese. Genomic DNA was extracted from peripheral blood leukocytes, and variants in the VAV2 and VAV3 genes were amplified by polymerase chain reaction (PCR) and directly sequenced. Two variants were identified: rs2156323 in VAV2 and rs2801219 in VAV3. The variants and the prevalence of POAG, NTG, and DG in unrelated Japanese patients indicated that the variants were not involved in the pathogenesis of POAG, NTG, or DG.

© 2013 Elsevier Inc. All rights reserved.

### 1. Introduction

Glaucoma is a complex, heterogeneous disease characterized by a progressive degeneration of the optic nerve axons, and it is the second highest cause of blindness, affecting approximately 70 million people worldwide [1]. Because the optic nerve axons degenerate in eyes with glaucoma, visual field defects develop. Primary open-angle glaucoma (POAG), the most common type of glaucoma, is associated with elevated intraocular pressure (IOP). Patients with POAG who have IOP in the normal range (<22 mmHg) are classified as having normal tension glaucoma (NTG) [2]. The prevalence of NTG is significantly higher among the Japanese than among Caucasians [3,4].

Although the precise molecular basis of POAG has not been established, it is most likely a genetically heterogeneous disorder caused by the interaction of multiple genes and environmental factors [5,6]. Several genetic loci that contribute to susceptibility to POAG have been identified. To date, at least 15 loci (GLC1A to GLC1O) have been linked to POAG, and three genes have been iden-

tified: the myocilin (*MYOC*) gene [7], the optineurin (*OPTN*) gene [8], and the WD-repeat domain 36 (*WDR36*) gene [9]. The *MYOC* gene encodes for myocilin and is mutated in juvenile-onset primary open-angle glaucoma. The optineurin (*OPTN*) gene is mutated in families with autosomal dominant, adult-onset POAG, including some with normal tension glaucoma. The *WDR36* gene is a relatively new causative gene for adult-onset POAG. However, several studies have reported that the *OPTN* and *WDR36* variants do not predispose subjects to POAG/NTG [10–15].

Recently, the genes for vav 2 guanine nucleotide exchange factor (VAV2) (OMIM 600428) and vav 3 guanine nucleotide exchange factor (VAV3) (OMIM 605541) were reported to cause POAG in the Japanese [10]. The authors provided functional evidence suggesting that *Vav2*- and *Vav2/Vav3*- deficient mice had a spontaneous glaucoma phenotype resulting in progressive iridocorneal changes and elevated IOPs. In addition, a genome-wide association study (GWAS) that screened for glaucoma susceptibility loci using single nucleotide polymorphism (SNP) analysis identified intronic SNPs in VAV2 (rs2156323) and VAV3 (rs2801219) as candidates for genes associated with POAG in Japanese glaucoma patients.

An accurate diagnostic test for pre-symptomatic individuals at risk for glaucoma is needed, and screening for the VAV2 and VAV3 genes may identify pre-symptomatic cases in the general population. Thus, the purpose of this study was to determine

\* Corresponding author at: Department of Ophthalmology, The Fourth Affiliated Hospital, China Medical University, 11 Xinhua Road, Heping District, Shenyang, Liaoning 110005, China. Fax: +86 24 62689311.

E-mail addresses: [locust.stone@hotmail.com](mailto:locust.stone@hotmail.com), [shidong@mail.cmu.edu.cn](mailto:shidong@mail.cmu.edu.cn) (D. Shi).

whether variants in the *VAV2* and *VAV3* genes contribute to POAG, NTG, and developmental glaucoma (DG) in Japanese patients.

## 2. Patients and methods

### 2.1. Patients

One hundred and sixty eight unrelated Japanese patients with POAG (89 men and 79 women; mean age  $63.6 \pm 14.4$  years), 163 unrelated Japanese patients with NTG (86 men and 77 women; mean age  $61.8 \pm 13.7$  years), and 45 unrelated Japanese patients with DG (18 men and 27 women; mean age  $30.7 \pm 10.7$  years), who were diagnosed in the ophthalmology clinic at the Tohoku University Hospital, Sendai, Japan, were studied. The percentages of patients from each of the different regions of Japan were as follows: 70% of the patients were from the northern region, 20% were from the eastern region, and <10% were from the western region of Japan.

The purpose and procedures of the experiment were explained to all the patients, and their informed consent was obtained. The procedures used conformed to the tenets of the Declaration of Helsinki, and the Tohoku University Institutional Review Board approved this study.

Routine ophthalmic examinations were performed on all the patients. The criteria for classifying a patient as having POAG were the following: (1) applanation IOP >22 mmHg in each eye; (2) glaucomatous cupping in each eye, including a cup-to-disc ratio >0.7; (3) visual field defects, determined by Goldmann and/or Humphrey perimetry, that are consistent with glaucomatous cupping in at least one eye; and (4) an open anterior chamber angle. The criteria for NTG were the following: (1) applanation IOP less than 22 mmHg in both eyes at each examination; and (2) the same characteristics as the POAG group. Patients with glaucoma due to secondary causes, e.g., trauma, uveitis, or steroid use, were excluded.

Control subjects (95 men and 85 women; mean age  $68.0 \pm 7.7$  years) were characterized by the following characteristics: (1) IOP <22 mmHg; (2) normal optic discs; and (3) no family history of glaucoma. To decrease the chance of including individuals with pre-symptomatic glaucoma in this group, we studied individuals who were older than 60.

### 2.2. Sample preparation and variant screening

Genomic DNA was extracted from peripheral blood leukocytes and purified using the Qiagen QIAamp Blood Kit (Qiagen, USA). The SNPs rs2156323 (*VAV2*) and rs2801219 (*VAV3*) and their flanking regions were amplified by polymerase chain reaction (PCR) using 0.5  $\mu$ M intronic primers in an amplification mixture (25  $\mu$ l) containing 0.2 mM dNTPs and 0.5 U Ex Taq polymerase (Takara), with the addition of 30 ng of template DNA at an annealing temperature of 60°C. The oligonucleotides for amplification and sequencing were selected using Primer3 software ([http://frodo.wi.mit.edu/cgi-bin/primer3/primer3\\_www.cgi/](http://frodo.wi.mit.edu/cgi-bin/primer3/primer3_www.cgi/), Massachusetts Institute of Technology, Cambridge, MA).

The PCR fragments were purified with ExoSAP-IT (USB, Cleveland, Ohio, USA) and were sequenced with the BigDye™ Terminator Cycle Sequencing Ready Reaction Kit (Perkin-Elmer, Foster City, California, USA) on an automated DNA sequencer (ABI PRISM™ 3100 Genetic Analyzer, Perkin-Elmer).

### 2.3. Statistical analyses

Differences in the genotype frequencies among the cases and controls were tested using Fisher's exact test, depending on the cell counts. Odds ratios (approximating relative risk) were calculated

to measure the association between the WDR36 genotype and the POAG/NTG phenotype, and the effects of the mutant allele were assumed to be dominant (wild/wild vs. wild/mutant and mutant/mutant combined). For each odds ratio, a *P* value and the 95% confidence intervals were calculated. The inferred haplotypes and LD, expressed as *D'* [11] and quantified between all pairs of biallelic loci, were estimated using the SNPalyze program version 4.0 (Dynacom, Yokohama, Japan). The significance of the associations was determined by contingency table analysis using the chi-square test or Fisher's exact test. The Hardy–Weinberg equilibrium was analyzed using the gene frequencies obtained by simple gene counting and the chi-square test with Yates' correction for comparing observed and expected values. For general stand-alone statistical power analysis, we used G\*Power [12]. G\*Power computes the power values for given sample sizes, effect sizes, and alpha levels (post hoc power analyses), and the sample sizes for given effect sizes, alpha levels, and power values (a priori power analyses).

## 3. Results

### 3.1. Allelic frequencies for rs2156323 SNP in *VAV2* and rs2801219 SNP in *VAV3*

Two variants were identified: rs2156323 in *VAV2* and rs2801219 in *VAV3*. The allelic frequencies for rs2156323 in *VAV2* and rs2801219 in *VAV3* for POAG, NTG, DG, and the control subjects are presented in Table 1. The allele frequencies of rs2156323 in *VAV2* in the POAG, the NTG, and the DG groups were not significantly different from the control group (minor allele frequency 0.051, 0.049, 0.022 vs. 0.036, respectively; *P* = 0.35, 0.40, and 0.51, respectively). The allele frequency of rs2801219 in *VAV3* was also not significantly higher in the two groups than in the control group (minor allele frequency 0.211, 0.236, 0.244 vs. 0.197, respectively; *P* = 0.64, 0.22 and 0.32, respectively). The SNP adhered to the Hardy–Weinberg expectations (*P* > 0.05).

### 3.2. Genotype frequencies for rs2156323 SNP in *VAV2* and rs2801219 SNP in *VAV3*

The genotype frequencies for rs2156323 in *VAV2* and rs2801219 in *VAV3* are listed for the POAG, NTG, DG, and control subjects in Table 2. For rs2156323 in *VAV2*, the genotype frequency was not statistically higher in the POAG (*P* = 0.25), the NTG (*P* = 0.29), and the DG (*P* = 0.62) groups than in the control group (Table 2). For rs2801219 in *VAV3*, the genotype frequency was not statistically higher in the POAG (*P* = 0.90), the NTG (*P* = 0.07), and the DG

**Table 1**

*VAV2* and *VAV3* SNPs allele frequencies in patients with POAG, NTG and in controls in Japanese.

SNP	<i>VAV2</i> (rs2156323 A/G)		<i>P</i> -value
	G	A	
POAG ( <i>n</i> = 168)	0.949	0.051	0.35
NTG ( <i>n</i> = 163)	0.951	0.049	0.40
DG ( <i>n</i> = 45)	0.978	0.022	0.51
Control ( <i>n</i> = 180)	0.964	0.036	
	<i>VAV3</i> (rs2801219 A/C)		
	A	C	
POAG ( <i>n</i> = 168)	0.789	0.211	0.64
NTG ( <i>n</i> = 163)	0.764	0.236	0.22
DG ( <i>n</i> = 45)	0.756	0.244	0.32
Control ( <i>n</i> = 180)	0.803	0.197	

The significance of the association was determined by a contingency table analysis using the  $\chi^2$  test.

**Table 2**

Frequency of genotypes VAV2 and VAV3 gene in patients with POAG, NTG and in controls in Japanese.

	POAG (n = 168)	NTG (n = 163)	DG (n = 45)	Control (n = 180)
<b>VAV2 (rs2156323 A/G)</b>				
G/G	151 (89.9%)	147 (90.2%)	43 (95.6%)	168 (93.3%)
G/A	17 (10.1%)	16 (9.8%)	2 (4.4%)	11 (6.1%)
A/A	0 (0%)	0 (0%)	0 (0%)	1 (0.6%)
P value*	0.25	0.29	0.80	
<b>VAV3 (rs2801219 A/C)</b>				
A/A	108 (64.3%)	92 (56.4%)	25 (55.6%)	119 (66.1%)
A/C	49 (29.2%)	65 (39.9%)	18 (40.0%)	51 (28.3%)
C/C	11 (6.5%)	6 (3.7%)	2 (4.4%)	10 (5.6%)
P value*	0.90	0.07	0.32	

Data presented are number of patients, unless otherwise indicated. The asterisk indicates that the significance of the association was determined by a contingency table analysis using the  $\chi^2$  test.

( $P = 0.32$ ) groups than in the control group (Table 2). The SNP adhered to the Hardy–Weinberg expectations ( $P > 0.05$ ).

### 3.3. Dominant and recessive model for rs2156323 SNP in VAV2 and rs2801219 SNP in VAV3

The homozygotes for the rs2156323 SNP A/A were 0% in the glaucoma subjects, and 0.6% in the control subjects ( $P > 0.05$ ; Table 2). We analyzed the dominant and recessive model for the rs2801219 SNP in VAV3 (Table 3). There was also no significant difference between the subgroups of glaucoma and SNP rs2801219 in VAV3. However, in the NTG group,  $P$  was 0.06 for the dominant model.

## 4. Discussion

Obtaining evidence that candidate genes and gene variants are significantly associated with a specific disease is more biologically meaningful when the same associations are also found in different ethnic populations. The significant associations would then indicate that these genes play a role in the pathogenesis of the disease [13]. Our findings showed that the alleles rs2156323 (VAV2) and rs2801219 (VAV3) were not significantly associated with POAG in Japanese patients. These risk alleles were also not significantly associated with POAG or primary angle closure glaucoma (PACG) in Indian cohorts [13]. It has also been reported that the genotype frequencies at these loci were not significantly different among POAG, PACG, and control subjects in Indian cohorts [14].

The finding that *Vav2*-deficiency alone resulted in a glaucoma phenotype in mice suggested that the absence of *Vav2* is associated with the development of glaucoma in mice. However, our findings demonstrated that there was no significant association between the VAV2 SNP and POAG, NTG, and DG. In addition, the VAV2 SNP rs2156323 was not associated with these glaucoma phenotypes. Functionally, the *Vav2/Vav3*-deficient (*Vav2*<sup>-/-</sup>*Vav3*<sup>-/-</sup>) mice had buphthalmos and iridocorneal changes that altered the aqueous outflow that lead to elevated intraocular pressure. The optic nerve head cupping resembled that found in developmental glaucoma

and PACG. Thus, we hypothesized that VAV2 and VAV3 could be major candidate genes for developmental glaucoma in humans. However, our results showed that DG, POAG and NTG were not significantly associated with alleles rs2156323 (VAV2) and rs2801219 (VAV3) (Tables 1 and 2). We also compared the DG group with an age-matched young control group ( $n = 60$ ;  $30.4 \pm 6.2$  years). Neither the frequencies of the A allele of VAV2 rs2156323 (DG 0.022 and young controls 0.075;  $P = 0.09$ , chi-square test), nor the C allele of rs2801219 (DG 0.244 and young controls 0.175;  $P = 0.22$ , chi-square test) was significantly different from young controls (data not shown).

There is a possibility that the lack of significant associations at these loci in our POAG cases could have been due to clinical heterogeneity.

Another possibility for the lack of significant associations is the sample size because small sample sizes are known to cause a type II error. There were 45 DG cases and 180 controls for a total of 225 subjects. For an effect size = 0.3 (medium), an  $\alpha$  error probability of 0.05, and a degree of freedom (Df) = 2, the power (1 – beta error probability) is 98.6%. However, for an effect size = 0.1 (small), an  $\alpha$  error probability of 0.05, and a Df = 2, the power is only 24.9%. To obtain a power of 80% under the same conditions, the total sample size must be 964 cases.

The Vav family of proteins consists of a group of signal transduction molecules with oncogenic potential that play important roles in development and cell signaling. The best known function of the Vav proteins is their role as GDP/GTP exchange factors that activate Rho guanosine triphosphatases (GTPases) in a phosphorylation-dependent manner [15]. In addition to their function as exchange factors, the evidence increasingly suggests that Vav proteins can mediate other cellular functions, most likely as adaptor molecules. Deregulation of the GDP/GTP exchange is one possible mechanism for the alterations that lead to iridocorneal angle closure. Thus, we suggest that VAV2 and VAV3 may still be candidate genes for PACG, and the association between *Vav2/Vav3* and PACG deserves further study.

In summary, the variants rs2156323 in the VAV2 gene and rs2801219 in the VAV3 gene do not appear to be major risk factors for the pathogenesis of glaucoma in the Japanese. However, *Vav2/Vav3*

**Table 3**

Frequency of genotypes in dominant or recessive model in VAV3 gene in patients with POAG, NTG and in controls in Japanese.

VAV3 (rs2801219 A/C)		POAG (n = 168)	NTG (n = 163)	DG (n = 45)	Control (n = 180)
Dominant	A/A	108 (64.3%)	92 (56.4%)	25 (55.6%)	119 (66.1%)
	A/C + C/C	60 (35.7%)	71 (43.6%)	20 (44.4%)	61 (33.9%)
P value*		0.72	0.06	0.19	
Recessive	A/A + A/C	157 (93.5%)	157 (96.3%)	43 (95.6%)	170 (94.4%)
	C/C	11 (6.5%)	6 (3.7%)	2 (4.4%)	10 (5.6%)
P value*		0.70	0.41	0.77	

Data presented are number of patients, unless otherwise indicated. The asterisk indicates that the significance of the association was determined by a contingency table analysis using the  $\chi^2$  test.

Vav3-deficient mice can still serve as useful models for the study of spontaneous glaucoma, and investigations into the development of the phenotype may provide information on the pathogenesis of glaucoma in humans.

## Disclosure

D. Shi, None; Y. Takano, None; M.T. Nakazawa, None; Mengke-gale, None; S. Yokokura, None; K. Nishida, None; N. Fuse, None.

## Acknowledgments

The authors thank Dr. Duco I. Hamasaki for editing the manuscript. This study was supported in part by a Grant-In-Aid for Scientific Research from the Ministry of Education, Science, and Culture of the Japanese Government (NF; C-22591928), by grant from the Ministry of Health, Labor, and Welfare of Japan to N.F., and by a grant from the Japan-China Medical Association to D.S.

## References

- [1] H.A. Quigley, Number of people with glaucoma worldwide, *Br. J. Ophthalmol.* 80 (1996) 389–393.
- [2] D. Gupta, *Glaucoma diagnosis and management*, Lippincott Williams & Wilkins, Philadelphia, 2005.
- [3] Y. Shiose, Y. Kitazawa, S. Tsukahara, T. Akamatsu, K. Mizokami, R. Futa, H. Katsushima, H. Kosaki, Epidemiology of glaucoma in Japan – a nationwide glaucoma survey, *Jpn. J. Ophthalmol.* 35 (1991) 133–155.
- [4] A. Iwase, Y. Suzuki, M. Araie, T. Yamamoto, H. Abe, S. Shirato, Y. Kuwayama, H.K. Mishima, H. Shimizu, G. Tomita, Y. Inoue, Y. Kitazawa, The prevalence of primary open-angle glaucoma in Japanese: the Tajimi Study, *Ophthalmology* 111 (2004) 1641–1648.
- [5] V. Raymond, Molecular genetics of the glaucomas: mapping of the first five “GLC” loci, *Am. J. Hum. Genet.* 60 (1997) 272–277.
- [6] M. Sarfarazi, Recent advances in molecular genetics of glaucomas, *Hum. Mol. Genet.* 6 (1997) 1667–1677.
- [7] E.M. Stone, J.H. Fingert, W.L. Alward, T.D. Nguyen, J.R. Polansky, S.L. Sunden, D. Nishimura, A.F. Clark, A. Nystuen, B.E. Nichols, D.A. Mackey, R. Ritch, J.W. Kalenak, E.R. Craven, V.C. Sheffield, Identification of a gene that causes primary open angle glaucoma, *Science* 275 (1997) 668–670.
- [8] T. Rezaie, A. Child, R. Hitchings, G. Brice, L. Miller, M. Coca-Prados, E. Heon, T. Krupin, R. Ritch, D. Kreutzer, R.P. Crick, M. Sarfarazi, Adult-onset primary open-angle glaucoma caused by mutations in optineurin, *Science* 295 (2002) 1077–1079.
- [9] S. Monemi, G. Spaeth, A. DaSilva, S. Popinchalk, E. Ilitchev, J. Liebmman, R. Ritch, E. Heon, R.P. Crick, A. Child, M. Sarfarazi, Identification of a novel adult-onset primary open-angle glaucoma (POAG) gene on 5q22.1, *Hum. Mol. Genet.* 14 (2005) 725–733.
- [10] K. Fujikawa, T. Iwata, K. Inoue, M. Akahori, H. Kadotani, M. Fukaya, M. Watanabe, Q. Chang, E.M. Barnett, W. Swat, VAV2 and VAV3 as candidate disease genes for spontaneous glaucoma in mice and humans, *PLoS One* 5 (2010) e9050.
- [11] J.H. Zhao, D. Curtis, P.C. Sham, Model-free analysis and permutation tests for allelic associations, *Hum. Hered.* 50 (2000) 133–139.
- [12] F. Faul, E. Erdfelder, A.G. Lang, A. Buchner, G\*Power 3: a flexible statistical power analysis program for the social, behavioral, and biomedical sciences, *Behav. Res. Methods* 39 (2007) 175–191.
- [13] S.J. Chanock, T. Manolio, M. Boehnke, E. Boerwinkle, D.J. Hunter, G. Thomas, J.N. Hirschhorn, G. Abecasis, D. Altshuler, J.E. Bailey-Wilson, L.D. Brooks, L.R. Cardon, M. Daly, P. Donnelly, J.F. Fraumeni Jr., N.B. Freimer, D.S. Gerhard, C. Gunter, A.E. Guttmacher, M.S. Guyer, E.L. Harris, J. Hoh, R. Hoover, C.A. Kong, K.R. Merikangas, C.C. Morton, L.J. Palmer, E.G. Phimister, J.P. Rice, J. Roberts, C. Rotimi, M.A. Tucker, K.J. Vogan, S. Wacholder, E.M. Wijsman, D.M. Winn, F.S. Collins, Replicating genotype–phenotype associations, *Nature* 447 (2007) 655–660.
- [14] K.N. Rao, I. Kaur, R.S. Parikh, A.K. Mandal, G. Chandrasekhar, R. Thomas, S. Chakrabarti, Variations in NTF4, VAV2, and VAV3 genes are not involved with primary open-angle and primary angle-closure glaucomas in an Indian population, *Invest. Ophthalmol. Vis. Sci.* 51 (2010) 4937–4941.
- [15] X.R. Bustelo, Vav proteins, adaptors and cell signaling, *Oncogene* 20 (2001) 6372–6381.